Analytical Biochemistry 408 (2011) 297–303

Contents lists available at ScienceDirect

Analytical Biochemistry

journal homepage: www.elsevier.com/locate/yabio

Vitamin B_{12} incorporated with multiwalled carbon nanotube composite film for the determination of hydrazine

Yogeswaran Umasankar, Tzu-Yen Huang, Shen-Ming Chen *

Department of Chemical Engineering and Biotechnology, National Taipei University of Technology, Taipei 106, Taiwan

ARTICLE INFO

Article history:
Received 16 July 2010
Received in revised form 26 September 2010
Accepted 27 September 2010
Available online 16 October 2010

Keywords:
Multiwalled carbon nanotubes
Vitamin B_{12}
Cobalamin
Modified electrodes
Electrocatalysis
Hydrazine

ABSTRACT

Electrochemically active composite film containing multiwalled carbon nanotubes (MWCNTs) and vitamin B_{12} was synthesized on glassy carbon, gold, and indium tin oxide electrodes by the potentiodynamic method. The presence of MWCNTs in the composite film (MWCNT–B_{12}) modified electrode mediates vitamin B_{12}'s redox reaction, whereas vitamin B_{12}'s redox reaction does not occur at bare electrode. The electrochemical impedance spectroscopy studies reveal that MWCNTs present in MWCNT–B_{12} film enhance electron shuttling between the reactant and electrode surface. The surface morphology of bare electrode, MWCNT film. and MWCNT–B_{12} composite film was studied using atomic force microscopy, which reveals vitamin B_{12} incorporated with MWCNTs. The MWCNT–B_{12} composite film exhibits promising enhanced electrocatalysis toward hydrazine. The electrocatalysis response of hydrazine at MWCNT film and MWCNT–B_{12} composite film was measured using cyclic voltammetry and amperometric current–time (i–t) curve techniques. The linear concentration range of hydrazine obtained at MWCNT–B_{12} composite film using the i–t curve technique is 2.0 μM–1.95 mM. Similarly, the sensitivity of MWCNT–B_{12} composite film for hydrazine determination using the i–t curve technique is 1.32 mA mM^{-1} cm^{-2}, and the hydrazine's limit of detection at MWCNT–B_{12} composite film is 0.7 μM.

Vitamin B_{12} or cobalamin is an organometallic cofactor with a complex structure [1]. The core structure of cobalamin includes the corrin ring with a central cobalt ion and the nucleotide loop with 50,60-dimethyl-benzimidazole base coordinated to cobalt at the lower axial position. Cobalamin with the backbone structure may contain different active groups such as water, cyanide, and histidine coordinated to cobalt at the upper axial position. The catalysis of reactions such as methylation and isomerization is driven by the conversion of cobalamin to its cofactor inside the animal cell [2]. A literature survey shows that vitamin B_{12}'s electrochemical property has been studied and reported [3,4]. These reports reveal that vitamin B_{12} exhibits a rich redox chemistry centered on the cobalt atom, where the Co^{III} in the vitamin B_{12} can be reduced reversibly to Co^{II} and further reduced to Co^{I}. Many reports also show that vitamin B_{12} adsorbs on electrode surfaces and can be used for oxidation or reduction reactions [5–7]. Therefore, immobilization of vitamin B_{12} on an electrode is a potential method for developing electrochemical sensor devices.

On the other hand, a wide variety of matrices made of carbon nanotubes (CNTs)[1] on the electrode surface for the detection of bioorganic and inorganic compounds are in the literature [8–11]. The rolled-up graphene sheets of carbon (i.e., CNTs) exhibit a π-conjugative structure with a highly hydrophobic surface. This property of CNTs allows them to interact with organic aromatic compounds through π–π electronic and hydrophobic interactions [12–14]. These interactions have been used for preparing composite sandwiched films for electrocatalysis studies [15] and in the designing of nanodevices [16]. Attempts have also been made to prepare hydrophilic surface CNTs to overcome the dispersion problem in aqueous medium for bioelectrochemical applications [17]. Electrodes modified with composite films are widely used in capacitors, batteries, fuel cells, chemical sensors, and biosensors [18–20]. Even though the electrocatalytic activity of CNTs or protein matrices individually showed good results, some properties such as mechanical stability, sensitivity for different techniques, and electrocatalysis of some compounds are poor. Therefore, in this work, an attempt was made to prepare a composite film made of CNTs and vitamin B_{12}. A previous report also

* Corresponding author. Fax: +886 2270 25238.
E-mail address: smchen78@ms15.hinet.net (S.-M. Chen).

[1] *Abbreviations used:* CNT, carbon nanotube; GCE, glassy carbon electrode; MWCNT, multiwalled carbon nanotube; PBS, phosphate buffer solution; CV, cyclic voltammetry; EQCM, electrochemical quartz crystal microbalance; EIS, electrochemical impedance spectroscopy; AFM, atomic force microscopy; i–t curve, current–time curve; LOD, limit of detection.

0003-2697/$ - see front matter © 2010 Elsevier Inc. All rights reserved.
doi:10.1016/j.ab.2010.09.037

reveals that the Co ligand form of vitamin B_{12} is a highly efficient nucleophile that can be used for carbon–carbon bond formation [21].

Hydrazine is a colorless liquid compound and a human carcinogen [22,23]. Hydrazine is also a powerful reducing agent and widely used in industrial applications as a reagent and catalyst. Other applications of hydrazine include insecticides, manufacture of metal films, and pharmaceutics. Because of its wide use in the environment, the detection and determination of hydrazine becomes essential. In the past, various determination methods have been developed for the detection of hydrazine [24–29]. For example, Zhou and Wang reported picomole-level detection of hydrazine using the liquid chromatography technique [30]. However, development of more sensitive and speedy determination methods is necessary. Even some electrochemical methods have limitations; for example, unmodified electrodes such as glassy carbon electrode (GCE) have a pronounced fouling effect, poor selectivity, and poor reproducibility. To overcome these limitations and enhance the electrocatalysis reaction of hydrazine, electrodes have been modified using catalysts such as ZnO nanostructures [31,32], gold nanoparticles [33], and nickel hexacyanoferrate [34]. To further improve the hydrazine determination efficiency, in this work a composite film made of multiwalled carbon nanotubes (MWCNTs) incorporated with vitamin B_{12} (MWCNT–B_{12}) was prepared and studied. MWCNT–B_{12} composite film's characterization, peak current, and electrocatalysis activity are reported along with its application in the determination of hydrazine. The MWCNT–B_{12} composite film formation processing involves the modification of electrode with uniformly well-dispersed MWCNTs followed by modification with vitamin B_{12}.

Materials and methods

Materials

Vitamin B_{12}, MWCNTs (o.d. = 7–15 nm, i.d. = 3–6 nm, length = 0.5–200 μm), and hydrazine obtained from Aldrich and Sigma–Aldrich (USA) were used as received. All other used chemicals were of analytical grade. The preparation of aqueous solution was done with twice distilled deionized water. Solutions were deoxygenated by purging with prepurified nitrogen gas. Phosphate buffer solution (PBS, pH 7.0) was prepared from 0.1 M Na_2HPO_4 and 0.1 M NaH_2PO_4 aqueous solutions.

Apparatus

Cyclic voltammetry (CV) was performed using an analytical system model CHI-1205 potentiostat. A conventional three-electrode cell assembly consisting of an Ag/AgCl reference electrode and a Pt wire counter electrode were used for electrochemical measurements. The working electrode was GCE modified with either MWCNT film or MWCNT–B_{12} composite film. In all of the experimental results, potential is reported versus Ag/AgCl reference electrode. The working electrode used for the electrochemical quartz crystal microbalance (EQCM) measurement was an 8-MHz AT-cut quartz crystal coated with gold electrode. The diameter of the quartz crystal is 13.7 mm, and the diameter of the gold electrode is 5 mm. Electrochemical impedance spectroscopy (EIS) measurements were performed using an IM6ex system (Zahner Elektrik, Germany). The morphological characterizations of various films were examined by means of atomic force microscopy (AFM, CSPM4000 microscope, Being Nano-Instruments, China). Amperometric current–time (i–t) curve measurements were performed using a CHI-750 potentiostat with an analytical rotator (AFMSRX, Pine Instruments, USA). All of the measurements were carried out at 25 ± 2 °C.

Preparation of MWCNT–B_{12} composite film modified electrode

The important challenge in the preparation of MWCNT solution for electrode modification was the difficulty in dispersing it into a homogeneous solution. In general, the dispersion of CNTs was carried out by physical (milling) and chemical methods (covalent and noncovalent functionalization). Briefly, by following a previously reported method [35,36], 50 mg of MWCNTs was heated at 350 °C for 2 h to remove the amorphous carbon and catalyst impurities and then was cooled to room temperature. The heat-treated MWCNTs were ultrasonicated for 4 h in 20 ml of concentrated HCl to remove other impurities and were washed several times with water and then dried at 100 °C in an air oven. These purified and dried MWCNTs were acid treated using sulfuric acid and nitric acid (3:1) by 6 h of ultrasonication at room temperature and then were washed several times with water until the pH of the supernatant was neutral. These acid-treated MWCNTs were dried overnight at 60 °C. Finally, the uniform dispersion of MWCNTs was obtained by 6 h of ultrasonication of acid-treated MWCNTs in water.

Before starting each experiment, GCEs were polished by a BAS polishing kit with 0.05 μm alumina slurry and then rinsed and ultrasonicated in double distilled deionized water. The GCEs studied were uniformly coated with 50 μg cm^{-2} MWCNTs and dried at room temperature. The electrochemical deposition of vitamin B_{12} on MWCNT modified GCE was performed from 0.5 mM vitamin B_{12} (in PBS) by consecutive cyclic voltammograms over a suitable potential region of 0.4 to −1.0 V with a scan rate of 50 mV s^{-1}. Then the MWCNT–B_{12} modified GCE was carefully washed with double distilled deionized water. The concentrations of homogeneously dispersed MWCNTs were measured exactly using a microsyringe.

Results and discussion

Electrodeposition of vitamin B_{12} at various electrodes and their characterizations

The electrochemical deposition of vitamin B_{12} (0.5 mM) on MWCNT modified GCE present in PBS was performed by consecutive cyclic voltammogram for the preparation of MWCNT–B_{12} composite film. The suitable potential range for vitamin B_{12} deposition is 0.4 to −1.0 V. On subsequent cycles, the cyclic voltammograms show redox peaks corresponding to vitamin B_{12} growing at MWCNT modified GCE (not shown). This above result indicates that during the cycle, deposition of vitamin B_{12} takes place on MWCNT modified GCE surface. The possible adsorption site of vitamin B_{12} at MWCNT is given in Scheme 1, where the minimum free energy is −4.07 kcal mol^{-1}. The docking of vitamin B_{12} on acid-treated MWCNTs was carried out using the Lamarckian genetic algorithm. The simulation conditions such as population size (50), maximum generations (3000), crossover rate (0.8), mutation rate (0.2), elitism (5), local search rate (0.06), and local search maximum steps (100) were kept constant, and the area around the binding site was varied to obtain the lowest free energy possible. The plot of binding site area versus free energy in Scheme 1 shows that the lowest free energy is obtained if the binding site area around MWCNTs is 135 nm^{-2}. The same plot shows that the free energy decreases while the binding site area increases until 135 nm^{-2}; however, the increase in binding site area higher than 135 nm^{-2} increases the free energy at the rate of 0.4 cal mol^{-1} nm^{-2}.

The above-prepared MWCNT–B_{12} composite film along with only MWCNT film was characterized using various electrochemical techniques in PBS. The vitamin B_{12} modified GCE was not included in the following studies because there is no deposition or redox reaction of vitamin B_{12} on bare GCE. Before transferring the

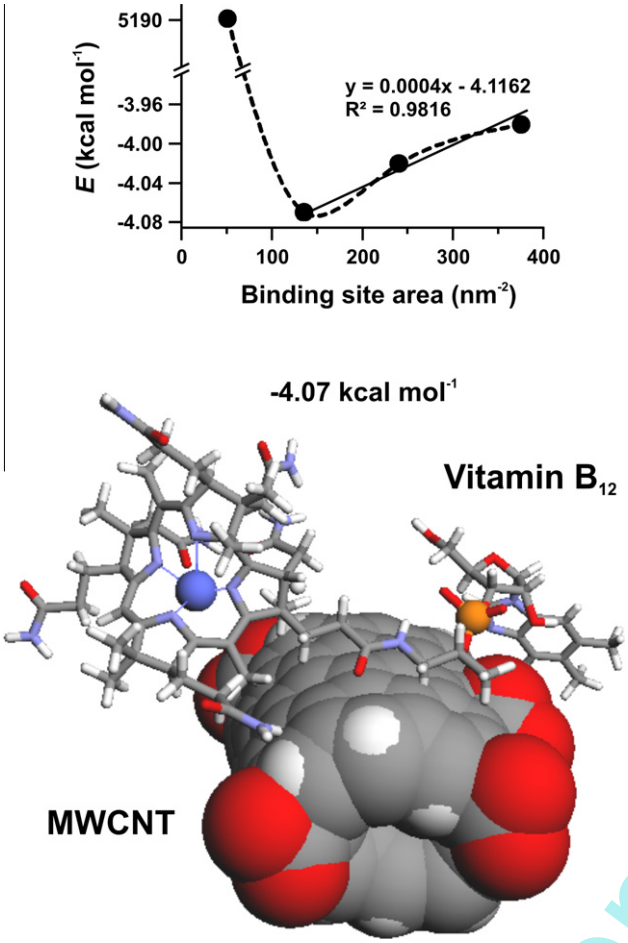

Scheme 1. Possible adsorption site of vitamin B_{12} at MWCNT given by Lamarckian genetic algorithm. The plot in the scheme shows the change in free energy with respect to binding site area.

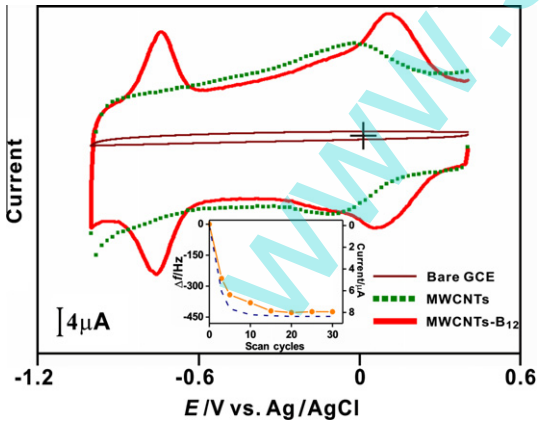

Fig.1. Cyclic voltammograms of bare GCE, MWCNT film modified GCE, and MWCNT–B_{12} composite film modified GCE in PBS (pH 7.0), potential scan between 0.4 and −1.0 V, with a scan rate of 20 mV s^{-1}. The inset is the plot of variation of frequency change (continuous line) and peak current change (dotted line) with the increase of scan cycles during the consecutive potential cyclic voltammograms of vitamin B_{12} at MWCNT-coated gold electrode (0.4 to −1.0 V with a scan rate of 20 mV s^{-1}).

MWCNT–B_{12} composite film into aqueous solution for electrochemical characterizations, the prepared film was washed carefully in deionized water to remove the loosely attached vitamin B_{12} present on the modified GCE. Fig. 1 shows the cyclic voltammograms of MWCNT–B_{12} composite film modified GCE, MWCNT film modified GCE (absence of vitamin B_{12}), and bare GCE in PBS. The corresponding cyclic voltammograms were measured at a scan rate of 20 mV s^{-1} in the potential range of 0.4 to −1.0 V. Among these three cyclic voltammograms, the $E^{0'}$ of redox couples of MWCNT–B_{12} are at −50.5 and 80.9 mV, respectively, where the redox couples represent the redox reaction of $Co^{III/II}$ and $Co^{II/I}$ present in vitamin B_{12} [37]. Similarly, the redox reaction of MWCNTs is represented by $E^{0'}$ = −70.7 mV.

The Epa, Epc, and Ipc values of MWCNT film and MWCNT–B_{12} composite film modified GCEs are given in Table 1. From the Ipc values, surface coverage concentration (Γ) of Co^{III} and Co^{II} species present in MWCNT–B_{12} composite film modified electrode is given in the table. The Γ of vitamin B_{12} was calculated using the equation $\Gamma = Q/nFA$, where Q is the charge involved in the reaction, n is the number of electrons transferred, F is the Faraday's constant, and A is the geometric area of the electrode. The Q values were calculated using CHI software, the geometric area of GCE is 0.08 cm^{-2}, and the number of electrons involved in vitamin B_{12} redox reactions is one each. The effective area of electrodes was also calculated using the Randles–Sevcik equation, and the values are 0.01 cm^{-2} for bare GCE, 0.02 cm^{-2} for MWCNT film modified GCE, and 0.02 cm^{-2} for MWCNT–B_{12} composite film modified GCE. These above results show that the presence of MWCNTs enhances the effective area of electrode by 2 μm^{-2} μg^{-1}.

EQCM studies of MWCNT–B_{12} composite film

The EQCM experiments were carried out by modifying the gold electrode of electrochemical quartz crystal by uniformly coating MWCNTs and then drying at 40 °C. The increase in voltammetric peak current of vitamin B_{12} redox couples and the frequency decrease (or mass increase) are found to be consistent with the growth of vitamin B_{12} film on MWCNT modified gold electrodes (figures not shown). These results also show that the obvious deposition potential started between 0.4 and −1.0 V. From the frequency change, the change in the mass of MWCNT–B_{12} composite film at the quartz crystal can be calculated by the Sauerbrey equation [1]; however, a 1-Hz frequency change is equivalent to 1.4 ng cm^{-2} mass change [38,39]. The mass change during vitamin B_{12} incorporation on MWCNT modified gold electrode for 30 cycles is 0.59 $\mu g\ cm^{-2}$. Similarly, from the voltammetric peak charge of Co^{III}, Γ of Co^{III} in vitamin B_{12} at MWCNT modified gold electrode for the 30th cycle is 0.57 nmol cm^{-2}. From the Γ value and by considering vitamin B_{12}'s molecular weight, the mass of vitamin B_{12} deposited on MWCNT modified gold electrode for 30 cycles was calculated to be 0.77 $\mu g\ cm^{-2}$. This mass change value obtained from the Γ result is consistent with the mass change value obtained from frequency change.

$$\text{mass change}(\Delta m) = -(1/2)(f_0^{-2})(\Delta f)A(K\rho)^{1/2}, \quad (1)$$

where f_0 is the oscillation frequency of the crystal, Δf is the frequency change. A is the area of the gold disk, K is the shear modulus of the crystal, and ρ is the density of the crystal. The inset of Fig. 1

Table 1
Epa, Epc, and Ipc values of redox reactions of MWCNTs and vitamin B_{12} and surface coverage concentration (Γ) of vitamin B_{12} at MWCNT modified GCE.

Modified electrode		Epa (mV)	Epc (mV)	Ipc (μA)	Γ (nmol cm^{-2})
Film	Species				
MWCNT	–	−25.4	−115.9	3.984	–
MWCNT–B_{12}	Co^{III}[a]	104.9	56.9	5.893	1.82
	Co^{II}[b]	−742.0	−759.0	9.443	1.67

[a] Co(III) to Co(II).
[b] Co(II) to Co(I).

shows the scan cycles versus current and frequency change plots of vitamin B_{12} deposition at MWCNT modified gold electrode. In this inset plots, the gross change in peak current of Co^{III} and the frequency shift over the course of the experiment are found to be consistent. These EQCM results show that the deposition of vitamin B_{12} takes places on MWCNT film.

AFM studies of bare electrode, MWCNT film, and MWCNT–B_{12} composite film

The MWCNT film and MWCNT–B_{12} composite film were prepared on indium tin oxide electrodes with similar conditions as mentioned in Materials and Methods. Then the bare electrode, MWCNT film, and MWCNT–B_{12} composite film modified electrodes were characterized using the AFM technique. The MWCNT film modified electrode shows uniformly deposited MWCNTs from a good dispersion solution (not shown). The uneven surface morphology in Fig. 2A is the bare electrode. The MWCNT–B_{12} composite film in Fig. 2B shows fibrous clusters of vitamin B_{12} formed over MWCNTs. Furthermore, in Fig. 2B, because of the deposition of vitamin B_{12} over MWCNTs, the uniform network of MWCNTs is not as clearly visible as in MWCNT film. Comparison of these AFM results in Fig. 2A and B reveals a significant morphological difference between modified and unmodified electrodes. The thickness of both MWCNT film and MWCNT–B_{12} composite film obtained using AFM results is 290 nm. However, in MWCNT–B_{12} composite film, bright clusters reveal slightly greater thickness of composite film compared with MWCNT film. These AFM results reveal the coexistence of MWCNTs and vitamin B_{12} as a composite film.

EIS studies of bare GCE, MWCNT film, and MWCNT–B_{12} composite film

Fig. 3 shows the impedance spectra represented as Nyquist plots (Z_{im} vs. Z_{re}) for bare GCE, MWCNT film modified GCE, and MWCNT–B_{12} composite film modified GCE in 5 mM $Fe(CN)_6^{3-/4-}$. The inset of Fig. 3 represents the Randles equivalent circuit model

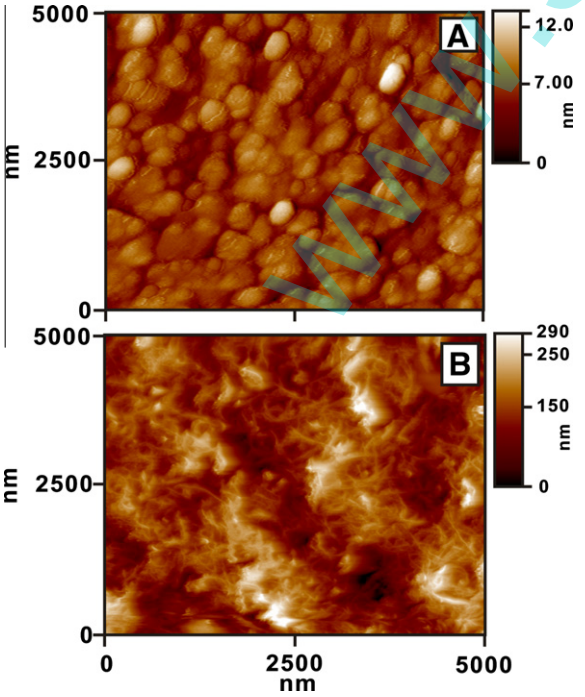

Fig.2. AFM images of bare electrode (A) and MWCNT–B_{12} composite film modified electrode (B).

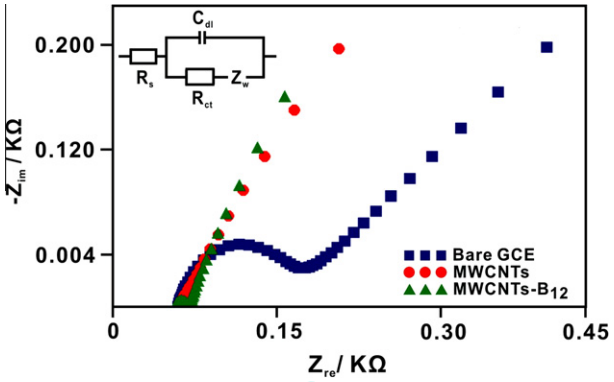

Fig.3. EIS of bare GCE, MWCNT film modified GCE, and MWCNT–B_{12} composite film modified GCE in 5 mM $Fe(CN)_6^{3-}/Fe(CN)_6^{4-}$ in PBS. Amplitude: 5 mV; frequency: 0.1 Hz to 1 MHz. The inset shows the Randles circuit for the above-mentioned electrodes.

used for fitting the experimental data, where R_s is electrolyte resistance, R_{et} is charge transfer resistance, C_{dl} is double layer capacitance, and Z_w is Warburg impedance. The semicircle appearing in the Nyquist plot indicates the parallel combination of charge transfer resistance and double layer capacitance resulting from electrode impedance [40]. All of the above-mentioned electrodes exhibit semicircles with various diameters in the frequency range of 0.1 Hz to 1 MHz. The EIS results show that the area of the semicircle for bare GCE is greater than that for MWCNT–B_{12} composite film, which is greater than that for MWCNT film. To find the electron transfer efficiency of the electrodes, R_{et} values were obtained for all modified and unmodified electrodes by fitting the above Nyquist plot results with the Randles equivalent circuit model. The obtained R_{et} values for bare GCE, MWCNT film, and MWCNT–B_{12} composite film are 104, 3.6, and 7.51 Ω, respectively. The above values reveal that the charge transfer resistance for MWCNT–B_{12} composite film is lower than that for bare GCE but higher than that for MWCNT film. This proves that MWCNTs present in MWCNT–B_{12} composite film enhance electron shuttling between reactant and the electrode surface.

Electrochemical signal of MWCNT–B_{12} composite film at different pH solutions

The effect of pH on MWCNT–B_{12} composite film was studied. Fig. 4 shows the cyclic voltammograms of MWCNT–B_{12} composite

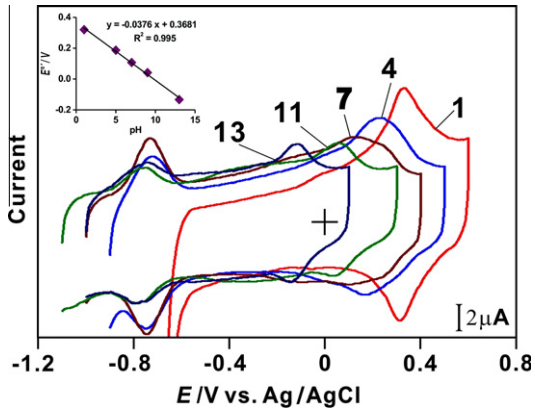

Fig.4. Cyclic voltammograms of MWCNT–B_{12} composite film modified GCE in various pH solutions (scan rate = 50 mV s^{-1}). The inset shows the formal potential versus pH from 1.0 to 13.0 (slope = −37 mV pH^{-1}), where the slope is almost closer to the Nernstian equation for nonequal number of electrons and protons transfer.

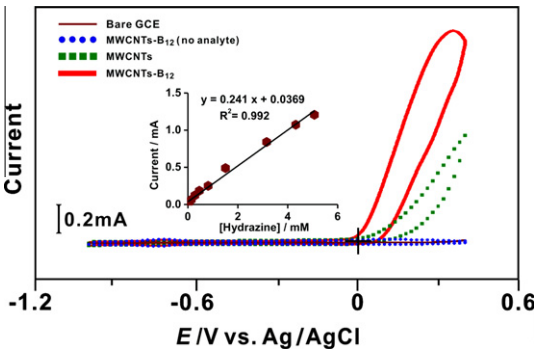

Fig.5. Cyclic voltammograms of hydrazine (5.1 mM) at bare GCE, MWCNT film modified GCE, and MWCNT–B_{12} composite film modified GCE in PBS at 50 mV s^{-1}, where MWCNT–B_{12} composite film is shown in both the presence and absence of 5.1 mM hydrazine. The inset is the plot of peak current versus hydrazine concentration at MWCNT–B_{12} composite film.

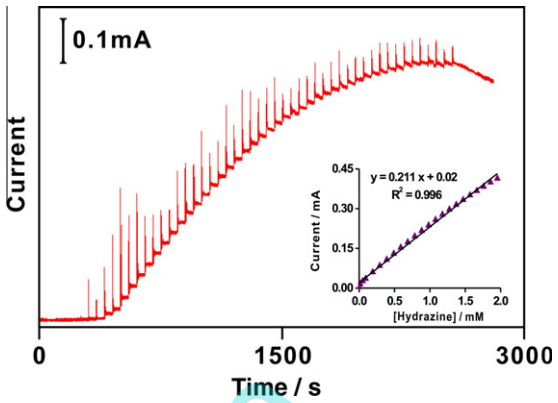

Fig.6. The *i–t* curve result of MWCNT–B_{12} composite film in PBS (at 1200 rpm and potential of 0.2 V) in the presence of hydrazine at 2.0 μM to 3.7 mM. The inset shows the plot of current versus different concentration of hydrazine obtained using the *i–t* curve at MWCNT–B_{12} composite film.

film modified GCE obtained in various pH aqueous buffer solutions without the presence of vitamin B_{12} in the solutions. In these above experiments the MWCNT–B_{12} composite film preparation was carried out in PBS as mentioned in Materials and Methods and then washed with deionized water before transferring it into various pH solutions. The results show that the redox reaction of $Co^{III/II}$ and $Co^{II/I}$ present in vitamin B_{12} is stable in the pH range between 4.0 and 13.0, whereas in pH 1.0 only $Co^{III/II}$ is active. Similarly, the $Co^{III/II}$ redox peak's Epa and Epc depend on the pH value of buffer solution, whereas the $Co^{II/I}$ redox peak's potentials do not depend on pH value. The response from the plot of $Co^{III/II}$ formal potential versus pH shows a slope of 37 mV pH^{-1}, which is close to that given by the Nernstian equation for nonequal number of electrons and proton transfer.

Electroanalytical response of hydrazine at MWCNT–B_{12} composite film

The MWCNT–B_{12} composite film was synthesized on GCE at similar conditions as given in Materials and Methods. Then the MWCNT–B_{12} composite film modified GCE was washed carefully in deionized water and transferred to PBS for the electrocatalysis of hydrazine. All of the cyclic voltammograms were recorded at a constant time interval of 1 min with N_2 purging before the start of each experiment. Fig. 5 shows the electrocatalytic oxidation of hydrazine (5.07 mM) at various film modified and unmodified GCEs with a scan rate of 50 mV s^{-1}. The various film modified GCEs tested were MWCNT film and MWCNT–B_{12} composite film, where the MWCNT–B_{12} composite film is shown with the highest concentration (5.07 mM) and in the absence of hydrazine. The cyclic voltammogram for MWCNT–B_{12} composite film exhibits reversible redox couples in the absence of hydrazine, and on the addition of hydrazine a new growth in the oxidation peak of hydrazine appears at Epa = 350 mV. In the above electrocatalysis experiment, an increase in concentration (2.08 μM to 5.07 mM) of hydrazine simultaneously produces a linear increase in oxidation peak current of hydrazine at MWCNT–B_{12} film with good film stability. However, there is no oxidation peak of hydrazine appearing at bare GCE and MWCNT film modified GCE even at 5.07 mM of hydrazine. It is obvious that only MWCNT–B_{12} composite film shows electrocatalytic activity for hydrazine when compared with bare GCE or MWCNT film modified GCE. This electrocatalytic activity in MWCNT–B_{12} composite film is due to the presence of vitamin B_{12}. From the slopes of linear calibration curves (Fig. 5 inset), the sensitivity of MWCNT–B_{12} composite film modified GCE toward hydrazine and its correlation coefficient were calculated to be 3.01 mA mM^{-1} cm^{-2} and 0.992, respectively. From the same results, hydrazine's limit of detection (LOD) at MWCNT–B_{12} composite film at a signal-to-noise ratio of 3 was calculated to be 0.7 μM. Various studies have shown that the inference of cations such as K^+, Na^+, Ca^{2+}, Mg^{2+}, Al^{3+}, Pb^{2+}, and Zn^{2+} does not affect hydrazine determination in real samples while using cobalt-containing complex modified electrodes [41]. Similarly, metal oxide modified electrodes also show negligible inference of the above cations during hydrazine determination [42]. The above reports reveal that the inference of cations during hydrazine determination by MWCNT–B_{12} composite film could be negligible.

Table 2
Comparison of electroanalytical results of hydrazine at various modified electrodes in various conditions.

Electrode	pH	Epa (V)	Linear range (μM)	Sensitivity	LOD (μM)	Reference
MWCNT–B_{12}	7.0	0.2	2–1950	1.32 mA mM^{-1} cm^{-2}	0.70	This work
CoPc/carbon paste	6.5	0.5	20–200	0.2 μA mM^{-1}	0.50	[29]
ZnO nanonails	7.4	−0.5 to 0.4	0.1–1.2	–	0.20	[31]
ZnO nanowires	7.4	−0.5 to 0.4	0.5–1.2	–	0.08	[32]
Au/PPy	7.0	0.14	1–500 and 500–7500	0.13 and 0.04 μA $μM^{-1}$	0.20	[33]
Nickel hexacyanoferrate	7.0	0.6	2–5000	0.26 μA $μM^{-1}$	2.28	[34]
Cobalt phthalocyanine	13.0	−0.2	125–980	I_{ap} = 1.47 + 4.90 × 10^5 (N_2H_4)	73.50	[41]
ZnO/MWCNTs	7.4	0.4	0.6–250	0.25 μA $μM^{-1}$	0.18	[42]
Mn^{II}/MWCNTs	8.0	0.4	1–1050	0.04 μA $μM^{-1}$	0.50	[43]
Hematoxylin/MWCNTs	7.0	0.22	2.0–122.8	0.02 μA $μM^{-1}$	0.68	[44]
BiHCF/CCEs	7.0	0.3	7.0–1010	4.2 μA $μM^{-1}$	3.00	[45]
Polymeric iron/tetraaminophthalocyanine	13.0	−0.2	1–100,000	–	–	[46]
Cobalt phthalocyanine/(PyC_6BPC_6Py)	13.0	−0.2	1–1000	2.4 nA $μM^{-1}$	0.60	[47]
Iron phthalocyanine/mercaptopyridine	7.0	0.35	13–92	9.40 × 10^{-3} μA $μM^{-1}$	5.00	[48]
CoTsPc multiplayer	13.0	0.2	2000–20,000	–	–	[49]

Fig. 6 is the amperometric response of MWCNT–B_{12} composite film in the *i–t* curve experiment with successive addition of hydrazine in the concentration range from 2.0 μM to 3.7 mM at the potential of 0.2 V and rotation rate of 1200 rpm. In these results, the amperometric response reaches approximately 5 s on the addition of hydrazine, and the response is proportional to its concentration. In this above *i–t* curve experiment, an increase in concentration (2.0 μM to 1.95 mM) of hydrazine simultaneously produces a linear increase in oxidation peak current of hydrazine at MWCNT–B_{12} composite film. However, after 1.95 mM, the rate of current increase started decreasing. From the slopes of linear calibration curves (Fig. 6 inset), the sensitivity of MWCNT–B_{12} composite film modified GCE toward hydrazine and its correlation coefficient were calculated to be 1.32 mA mM^{-1} cm^{-2} and 0.996, respectively. From the same results, hydrazine's LOD at MWCNT–B_{12} at a signal-to-noise ratio of 3 was calculated to be 0.7 μM. Comparison of the previously reported electroanalytical values (Table 2) with those of MWCNT–B_{12} composite film shows that the oxidation of hydrazine occurs at lower potential than in most electrodes. Furthermore, the linear range, sensitivity, and LOD of hydrazine at MWCNT–B_{12} composite film are better than those in most of the electrodes in Table 2. These results show that MWCNT–B_{12} composite film can be efficiently used for hydrazine determination.

Conclusions

Composite material containing MWCNTs and vitamin B_{12} at glassy carbon, gold, and indium tin oxide electrodes has been reported. The developed MWCNT–B_{12} composite film for electrocatalysis combines the advantages of ease of fabrication, high reproducibility, and sufficient stability. The AFM results showed the differences among bare electrode, MWCNT film, and MWCNT–B_{12} composite film morphology. Furthermore, it was found that MWCNT–B_{12} composite film has excellent functional property along with good electrocatalysis activity on hydrazine. The experimental methods of CV and the *i–t* curve with MWCNT–B_{12} composite film presented in this article provide an opportunity for qualitative and quantitative characterization of a hydrazine sensor. Therefore, this work establishes and illustrates in principle and potential a simple and novel approach for the development of a voltammetric and amperometric sensor based on modified GCE.

Acknowledgments

This work was supported by the National Science Council and the Ministry of Education of Taiwan (Republic of China).

References

[1] S.N. Fedosov, L. Berglund, E. Nexø, T.E. Petersen, Tetrazole derivatives and matrices as novel cobalamin coordinating compounds, J. Organometallic Chem. 692 (2007) 1234–1242.
[2] R. Baanerjee, S.W. Ragsdale, The many faces of vitamin B_{12}: catalysis by cobalamin-dependent enzymes, Annu. Rev. Biochem. 72 (2003) 209–247.
[3] B. Jaselkis, H. Diehl, The polarography of vitamins B_{12r} and B_{12a}, J. Am. Chem. Soc. 76 (1954) 4345–4348.
[4] R.H. Silvia, G.R. Gustavo, C.G. Héctor, Enhanced application of square wave voltammetry with glassy carbon electrode coupled to multivariate calibration tools for the determination of B_6 and B_{12} vitamins in pharmaceutical preparations, Talanta 61 (2003) 743–753.
[5] J.H. Zagal, M.J. Aguirre, C.G. Parodi, J. Sturm, Electrocatalytic activity of vitamin B_{12} adsorbed on graphite electrode for the oxidation of cysteine and glutathione and the reduction of cysteine, J. Electroanal. Chem. 374 (1994) 215–222.
[6] M.S. Lin, H.J. Leu, C.H. Lai, Development of vitamin B_{12} based disposable sensor for dissolved oxygen, Anal. Chim. Acta 561 (2006) 164–170.
[7] S. Dong, L. Chi, P. He, Q. Wang, Y. Fang, Simultaneous determination of antioxidants at a chemically modified electrode with vitamin B_{12} by capillary zone electrophoresis coupled with amperometric detection, Talanta 80 (2009) 809–814.
[8] U. Yogeswaran, S.M. Chen, Separation and concentration effect of *f*-MWCNTs on electrocatalytic responses of ascorbic acid, dopamine, and uric acid at *f*-MWCNTs incorporated with poly(neutral red) composite films, Electrochim. Acta 52 (2007) 5985–5996.
[9] G. Wu, Y.S. Chen, B.Q. Xu, Remarkable support effect of SWNTs in Pt catalyst for methanol electrooxidation, Electrochem. Commun. 7 (2005) 1237–1243.
[10] J. Wang, M. Musameh, Electrochemical detection of trace insulin at carbon-nanotube-modified electrodes, Anal. Chim. Acta 511 (2004) 33–36.
[11] J. Wang, M. Li, Z. Shi, N. Li, Z. Gu, Electrocatalytic oxidation of 3,4-dihydroxyphenylacetic acid at a glassy carbon electrode modified with single-wall carbon nanotubes, Electrochim. Acta 47 (2001) 651–657.
[12] Q. Li, J. Zhang, H. Yan, M. He, Z. Liu, Thionine-mediated chemistry of carbon nanotubes, Carbon 42 (2004) 287–291.
[13] J. Zhang, J.K. Lee, Y. Wu, R.W. Murray, Photoluminescence and electronic interaction of anthracene derivatives adsorbed on sidewalls of single-walled carbon nanotubes, Nano Lett. 3 (2003) 403–407.
[14] A. Star, T.R. Han, J. Christophe, P. Gabriel, K. Bradley, G. Gruner, Interaction of aromatic compounds with carbon nanotubes: correlation to the Hammett parameter of the substituent and measured carbon nanotube FET response, Nano Lett. 3 (2003) 1421–1423.
[15] M. Zhang, K. Gong, H. Zhang, L. Mao, Layer-by-layer assembled carbon nanotubes for selective determination of dopamine in the presence of ascorbic acid, Biosens. Bioelectron. 20 (2005) 1270–1276.
[16] R.J. Chen, Y. Zhang, D. Wang, H. Dai, Noncovalent sidewall functionalization of single-walled carbon nanotubes for protein immobilization, J. Am. Chem. Soc. 123 (2001) 3838–3839.
[17] Y. Yan, M. Zhang, K. Gong, L. Su, Z. Guo, L. Mao, Adsorption of methylene blue dye onto carbon nanotubes: a route to an electrochemically functional nanostructure and its layer-by-layer assembled nanocomposite, Chem. Mater. 17 (2005) 3457–3463.
[18] G. Han, J. Yuan, G. Shi, F. Wei, Electrodeposition of polypyrrole/multiwalled carbon nanotube composite films, Thin Solid Films 474 (2005) 64–69.
[19] U. Yogeswaran, S. Thiagarajan, S.M. Chen, Nanocomposite of functionalized multiwall carbon nanotubes with nafion, nano platinum, and nano gold biosensing film for simultaneous determination of ascorbic acid, epinephrine, and uric acid, Anal. Biochem. 365 (2007) 122–131.
[20] E. Frackowiak, V. Khomenko, K. Jurewicz, K. Lota, F. Béguin, Supercapacitors based on conducting polymers/nanotubes composites, J. Power Sources 153 (2006) 413–418.
[21] C.K. Njue, B. Nuthakki, A. Vaze, J.M. Bobbitt, J.F. Rusling, Vitamin B_{12}-mediated electrochemical cyclopropanation of styrene, Electrochem. Commun. 3 (2001) 733–736.
[22] T. Leakakos, R.C. Shank, Hydrazine genotoxicity in the neonatal rat, Toxicol. Appl. Pharmacol. 126 (1994) 295–300.
[23] H. Zheng, R.C. Shank, Changes in methyl-sensitive restriction sites of liver DNA from hamsters chronically exposed to hydrazine sulfate, Carcinogenesis 17 (1996) 2711–2717.
[24] E.A. Malaki, M.A. Koupparis, Kinetic study of the determination of hydrazines, isoniazid, and sodium azide by monitoring their reactions with 1-fluoro-2,4-dinitrobenzene, by means of a fluoride-selective electrode, Talanta 36 (1989) 431–436.
[25] H.M. Ji, W.Y. Hou, E.K. Wang, Amperometric flow-injection analysis of hydrazine by electrocatalytic oxidation at cobalt tetraphenylporphyrin modified electrode with heat treatment, Talanta 39 (1992) 45–50.
[26] H. Xia, H.L. Li, D.Q. Yang, Voltammetric determination of hydrazine based on catalytic reaction in the presence of 4-hydroxy-2,2,6,6-tetramethyl-piperdinyloxy (TEMPOL) radical, Electroanalysis 9 (1997) 1429–1431.
[27] A.M. ElBrashy, L.A. ElHussein, Colorimetric determination of some important hydrazine derivatives, Anal. Lett. 30 (1997) 609–622.
[28] J. Wang, M.P. Chatrathi, B.M. Tian, R. Polsky, Capillary electrophoresis chips with thick-film amperometric detectors: separation and detection of hydrazine compounds, Electroanalysis 12 (2000) 691–694.
[29] W. Siangproh, O. Chailapakul, R. Laocharoensuk, J. Wang, Microchip capillary electrophoresis/electrochemical detection of hydrazine compounds at a cobalt phthalocyanine modified electrochemical detector, Talanta 67 (2005) 903–907.
[30] J. Zhou, E. Wang, Electrocatalytic oxidation and flow detection of hydrazine compounds in liquid chromatography at a vitamin B-12 adsorbed glassy carbon electrode, Electroanalysis 4 (1992) 473–479.
[31] A. Umar, M.M. Rahman, S.H. Kim, Y-B. Hahn, Zinc oxide nanonail based chemical sensor for hydrazine detection, Chem. Commun. 2 (2008) 166–168.
[32] A. Umar, M.M. Rahman, Y-B. Hahn, Ultra-sensitive hydrazine chemical sensor based on high-aspect-ratio ZnO nanowires, Talanta 77 (2009) 1376–1380.
[33] J. Li, X. Lin, Electrocatalytic oxidation of hydrazine and hydroxylamine at gold nanoparticle-polypyrrole nanowire modified glassy carbon electrode, Sensors Actuat. B 126 (2007) 527–535.
[34] A. Salimi, K. Abdi, Enhancement of the analytical properties and catalytic activity of a nickel hexacyanoferrate modified carbon ceramic electrode prepared by two-step sol–gel technique: application to amperometric detection of hydrazine and hydroxyl amine, Talanta 63 (2004) 475–483.

[35] H. Su, R. Yuan, Y. Chai, Y. Zhuo, C. Hong, Z. Liu, X. Yang, Multilayer structured amperometric immunosensor built by self-assembly of a redox multi-wall carbon nanotube composite, Electrochim. Acta 54 (2009) 4149–4154.
[36] D.R.S. Jeykumari, S.S. Narayanan, A novel nanobiocomposite based glucose biosensor using neutral red functionalized carbon nanotubes, Biosens. Bioelectron. 23 (2008) 1404–1411.
[37] L. Ngandu, D. Robin, A. El Kasmi, D. Lexa, Vitamin B_{12}-transport protein interaction: electrochemistry of aquo- and glutathionyl-cobalamins adsorbed on carbon electrodes—role of the nucleotide chain, Inorg. Chim. Acta 292 (1999) 204–212.
[38] S.M. Chen, K-C. Lin, The electrocatalytic properties of polymerized neutral red film modified electrodes, J. Electroanal. Chem. 511 (2001) 101–114.
[39] S.M. Chen, M-I. Liu, Electrocatalytic properties of NDGA and NDGA/FAD hybrid film modified electrodes for NADH/NAD^+ redox reaction, Electrochim. Acta 51 (2006) 4744–4753.
[40] H.O. Finklea, D.A. Snider, J. Fedyk, Characterization of octadecanethiol-coated gold electrodes as microarray electrodes by cyclic voltammetry and AC impedance spectroscopy, Langmuir 9 (1993) 3660–3667.
[41] C. das D.C. Conceição, R.C. Faria, O. Fatibello-Filho, A.A. Tanaka, Electrocatalytic oxidation and voltammetric determination of hydrazine in industrial boiler feed water using a cobalt phthalocyanine-modified electrode, Anal. Lett. 41 (2008) 1010–1021.
[42] B. Fang, C. Zhang, W. Zhang, G. Wang, A novel hydrazine electrochemical sensor based on a carbon nanotube-wired ZnO nanoflower-modified electrode, Electrochim. Acta 55 (2009) 178–182.
[43] M.A. Kamyabi, O. Narimani, H.H. Monfared, Electrocatalytic oxidation of hydrazine using glassy carbon electrode modified with carbon nanotube and terpyridine manganese(II) complex, J. Electroanal. Chem. 644 (2010) 67–73.
[44] H.R. Zare, N. Nasirizadeh, Hematoxylin multi-wall carbon nanotubes modified glassy carbon electrode for electrocatalytic oxidation of hydrazine, Electrochim. Acta 52 (2007) 4153–4160.
[45] J. Zheng, Q. Sheng, L. Li, Y. Shen, Bismuth hexacyanoferrate-modified carbon ceramic electrodes prepared by electrochemical deposition and its electrocatalytic activity towards oxidation of hydrazine, J. Electroanal. Chem. 611 (2007) 155–161.
[46] P. Ardiles, E. Trollund, M. Isaacs, F. Armijo, J.C. Canales, M.J. Aguirre, M.J. Canales, Electrocataltyic oxidation of hydrazine at polymeric iron-tetraaminophthalocyanine modified electrodes, J. Mol. Catal. A 165 (2001) 169–175.
[47] C. Sun, Y. Sun, X. Zhang, X. Zhang, D. Jiang, Q. Gao, H. Xu, J. Shen, Fabrication of a multilayer film containing cobalt phthalocyanine on the surface of a gold electrode based on electrostatic interaction and its application as an amperometric sensor of hydrazine, Thin Solid Films 288 (1996) 291–295.
[48] K.I. Ozoemena, T. Nyokong, Electrocatalytic oxidation and detection of hydrazine at gold electrode modified with iron phthalocyanine complex linked to mercaptopyridine self-assembled monolayer, Talanta 67 (2005) 162–168.
[49] X. Li, S. Zhang, C. Sun, Fabrication of a covalently attached multilayer film electrode containing cobalt phthalocyanine and its electrocatalytic oxidation of hydrazine, J. Electroanal. Chem. 553 (2003) 139–145.